Geochemistry and bonding of thiospinel minerals

DAVID J. VAUGHAN
Department of Geology and Mineralogy, University of Oxford,
Oxford, England
and
ROGER G. BURNS and VIRGINIA MEE BURNS
Department of Earth and Planetary Sciences, Massachusetts Institute of
Technology, Cambridge, Massachusetts 02139

Abstract—The thiospinel group of minerals present a variety of interesting problems in mineral chemistry. Carrollite ($CuCo_2S_4$), linnaeite (Co_3S_4), siegenite [$(Co, Ni)_3S_4$], polydymite (Ni_3S_4) and violarite ($FeNi_2S_4$) occur in ore deposits, daubréelite [$(Fe, Mn, Zn)Cr_2S_4$] is present in meteorites and greigite (Fe_3S_4) is found in lacustrine sediments. This paper illustrates how the crystal chemistry, geochemistry and certain physical properties may be interpreted by molecular orbital and band theories of the chemical bond. In the spinel structure, transition metal ions occur in tetrahedral and octahedral coordinations, and 3d electrons of cations bonded to sulphur atoms are distributed amongst non-bonding and anti-bonding molecular orbitals. The composition ranges, geochemistry, and variations of cell parameters, microhardness, reflectivities and relative stabilities of thiospinels are directly related to the numbers of electrons in antibonding molecular orbitals.

Linnaeite, which is the most stable thiospinel mineral in the system Cu–Co–Ni–Fe–S, has the smallest number of antibonding electrons. It has the smallest cell edge, highest reflectivity and largest microhardness. With increasing electron occupancy of the antibonding orbitals, each of these physical properties, together with the thermal stabilities, decrease along the linnaeite–siegenite–polydymite, linnaeite–carrollite and violarite–polydymite series. In each of these minerals, the unusually small cell edge may be correlated with the occurrence of transition metal ions in low-spin states. The metallic conductivity and Pauli-paramagnetism of many of these minerals is related to electron delocalization in antibonding molecular orbitals.

Iron cations occur in high-spin states in greigite, giving rise to increased numbers of electrons in antibonding orbitals. As a result greigite has a larger cell edge and lower thermal stability than other thiospinel minerals. The semiconducting and ferrimagnetic properties of greigite indicate that the 3d electrons are more localized on the cation than sulphospinels in the Cu–Co–Ni–Fe–S system. Absence of solid-solution between violarite and greigite is attributed to differing spin-states of octahedral Fe(II) ions, which are low-spin in violarite and high-spin in greigite. The high thermal stability of daubréelite is due to the large octahedral site preference energy of Cr^{3+} in the structure.

The preference of transition metal ions for octahedral coordination is reflected by the ease in which thiospinel phases transform to a cation defect NiAs structure at elevated pressures and temperatures. As a result, polymorphic transitions involving thiospinel phases are postulated in the mantle and in shocked meteorites.

INTRODUCTION

A NUMBER of the sulphide phases of transition elements crystallize with the spinel structure (HULLIGER, 1968; TRESSLER et al., 1968). Thiospinels occur in a wide variety of geologic environments ranging from meteorites and hydrothermal vein deposits to low temperature lacustrine environments and soils. They occur in important ore deposits of cobalt, copper and nickel. Individual thiospinel minerals, however, tend to occur in a rather restricted geologic environment. Some characteristic occurrences of the individual minerals taken from the recent literature are summarized in Table 1.

Table 1. Formulae and occurrences of thiospinel minerals

Mineral	Formula	Examples of geologic occurrence	References
carrollite	$CuCo_2S_4$	An important cobalt ore in Katanga and Zambia. Usually found as disseminated anhedral grains and may be intimately intergrown with copper sulphides. At N'Kana Zambia, its main associates are chalcopyrite, bornite, chalcocite, pyrite, cattierite, cobaltian calcite, and asbolane or Co–Mn wad.	Andrews (1962)
daubréelite	$FeCr_2S_4$	Common accessory mineral in iron meteorites and highly reduced enstatite achondrites and chondrites. Closely associated with, and often exsolved from, troilite. In the Norton Co. achondrite it occurs with enstatite, olivine, kamacite, metallic copper, albandite and troilite.	Keil and Fredriksson (1963) Keil (1968)
greigite (melnikovite)	Fe_3S_4	Found in lacustrine and bottom sediments; mineralized vegetable debris. Also reported in hydrothermal veins associated with stibnite. At San Bernadino Co., California, occurs with montmorillonite, chlorite, calcite, colemanite, veatchite, orpiment, realgar and minor marcasite in fine laminae of blackish clays, interlaminated with sulphide-free clays, silts and sands in flat lying Tertiary lacustrine sediments.	Skinner et al. (1964) Polushkina and Sidorenko (1963) Kramm and Sukhitskaya (1965) Radusinović (1966) Jedwab (1967)
indite	$FeIn_2S_4$	Rare mineral found in colomorphous cassiterite deposit in Upper Cretaceous quartz porphyries at Dzalindin, U.S.S.R.; associated with quartz, cassiterite, jalindite, chalcopyrite, pyrite, arsenopyrite and mimetite.	Genkin and Murav'eva (1963) [Chem. Abstr. 59, 15032 h]
linnaeite	Co_3S_4	Possibly the most widespread of the thiospinel minerals. Reported in over a dozen countries. Found in mineable quantities at Katanga. Occurs in sulphide veins usually associated with chalcopyrite, pyrite and pyrrhotite. At Kilembe, Uganda, chalcopyrite, pyrite, pyrrhotite and linnaeite occur as long tabular masses in albite–quartz–granulites.	Andrews (1962)
polydymite	Ni_3S_4	Usually described as a low temperature secondary mineral in nickel deposits, but reported as primary in association with pyrite at Copper King Mine, Boulder County, Colorado.	Cornwall (1966) Goddard and Lovering (1942)

Table 1 (continued)

Mineral	Formula	Examples of geologic occurrence	References
siegenite	$(Co, Ni)_3S_4$	Best known occurrences are Siegen-land Westphalia and Fredericks-town, Missouri. At Frederickstown, it occurs in isolated patches of copper mineralization in this lead zinc area. The siegenite occurs as small disseminated crystals and veins following bedding contacts with Cambrian shaley carbonate country rock.	ANDREWS (1962) SNYDER and GERDEMANN (1969) CORNWALL (1966)
violarite	$FeNi_2S_4$	Normally occurs as a secondary mineral after pentlandite in the weathering zone of many nickel sulphide deposits, such as Sudbury, Ontario. Has been reported in hydrothermal vein deposits.	HAWLEY (1962) CORNWALL (1966) BIRD (1969)

Studies in solid state physics have shown that natural and synthetic thiospinels and analogous compounds display a diverse range of magnetic and electrical proper-ties (LOTGERING, 1956; BOUCHARD et al., 1965) which have been interpreted by band and molecular orbital theories (GOODENOUGH, 1967, 1969). The present paper applies these theories of the chemical bond to account for the composition ranges and the variations of cell parameters, microhardness, reflectivities and relative stabilities of thiospinel minerals.

COMPOSITIONS OF THIOSPINEL MINERALS

A review of the chemical compositions of Fe–Co–Ni–Cu thiospinels was published by TARR (1935) and extended by VOKES (1967). End member compositions include the minerals linnaeite Co_3S_4, polydymite Ni_3S_4, and greigite Fe_3S_4. The compound Cu_3S_4 is unknown and is unlikely to exist, since the Cu(III) oxidation state is extremely unstable. Intermediate compositions include the minerals carrollite $CuCo_2S_4$, violarite $NiFe_2S_4$, and siegenite $(Co, Ni)_3S_4$. Analogous chalcogenide minerals with the spinel structure include bornhardtite Co_3Se_4, trüstedtite Ni_3Se_4, selenolinnaeite $Co_3(S, Se)_4$, seleniosiegenite $(Co, Ni)_3 (S, Se)_4$, tyrrellite $(Cu, Co, Ni)_3Se_4$ and poly-dymite–trüstedtite solid-solutions $Ni_3(S, Se)_4$ (VUORELAINEN et al., 1964; HEY, 1962; FLEISCHER, 1966).

The chemical compositions of some thiospinel minerals taken from recent liter-ature are plotted in Fig. 1, which represents two triangles composing the Cu–Co–Ni–Fe tetrahedron (VOKES, 1967). The metal atoms in each analysis have been re-calculated into two groupings—Cu–Co–Ni and Co–Ni–Fe (each to 100 per cent)—so that each analysis is represented by two points, one in each triangle. Tielines, however, have been omitted in Fig. 1. Almost complete solid-solution appears to exist between Co_3S_4 and Ni_3S_4, with extensions into the Cu and Fe fields towards the compositions $CuCo_2S_4$ and $FeNi_2S_4$. Analyses exceeding 33% Cu in the Cu–Co–Ni triangle probably represent impurities of copper sulphides intimately intergrown with carrollite. Similarly, some of the siegenites and violarites may be contaminated by iron sulphides. No minerals with compositions $CuNi_2S_4$ and $FeCo_2S_4$ have been
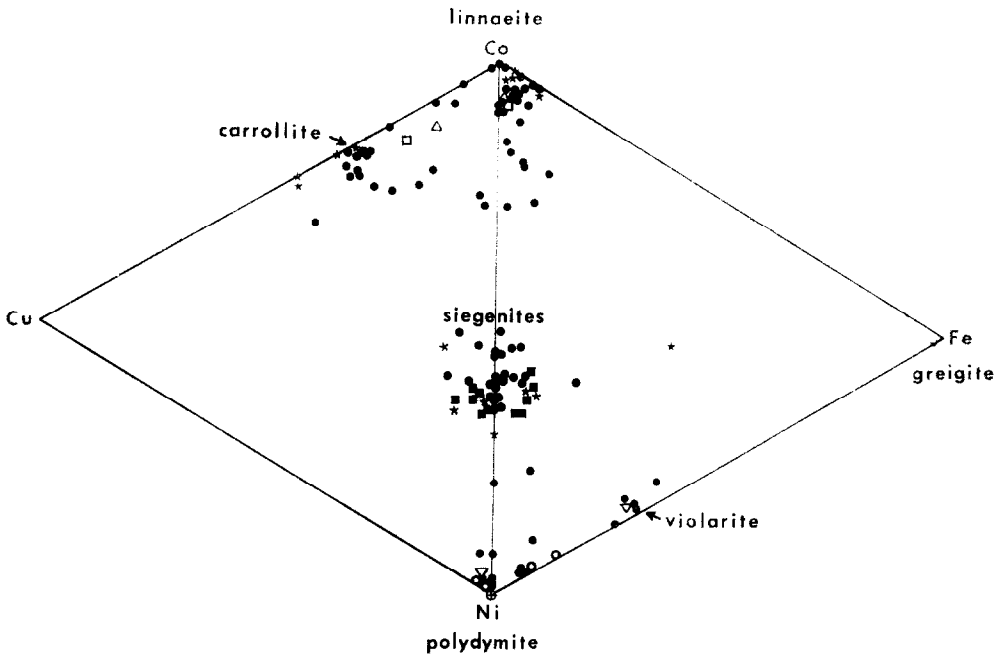
Fig. 1. Analysis of thiospinel minerals (after VOKES, 1967). The diagram consists of the Cu–Co–Ni and Co–Ni–Fe triangles in the Cu–Co–Ni–Fe tetrahedron. Each analysis is plotted in each of the triangles but tielines are omitted [see VOKES (1967) for tielines].

○ VOKES (1967); ★ POWELL (1967); △ KATITSYN (1959); □ PERMINGEAT and WEINRYB (1960); ■ HACH–ALI and OTTEMAN (1970); ▽ BIRD (1969); ⊕ FRENZEL and OTTEMAN (1968); ○ HOFFMAN et al. (1963).

reported, although synthetic phases with these compositions have been catalogued (HULLIGER, 1968). LOTGERING (1965) questioned his original synthesis of $FeCo_2S_4$. Negligible solid-solution exists between Fe_3S_4–Co_3S_4 and Fe_3S_4–$FeNi_2S_4$.

Several synthetic chromium thiospinels have been made, but only daubréelite $FeCr_2S_4$ has been found as a mineral, occurring in meteorites. Electron microprobe measurements of several meteorites have shown that daubréelite always contains a few per cent manganese. (EL GORESY and KULLERUD, 1969; KEIL and FREDRIKSSON, 1963). Some daubréelites also contain zinc (KEIL, 1968), and up to eight per cent zinc has been reported (EL GORESY, 1967). The rare mineral indite $FeIn_2S_4$ has been found in tin ores associated with quartz porphyries (GENKIN and MURAV'EVA, 1963).

Greigite, originally discovered in lacustrine sediments (SKINNER et al., 1964), has also been reported in hydrothermal veins where analyses indicate that it contains about 0·22% Ni (RADUSINOVIĆ, 1966). The composition Fe_3S_4 also occurs as the mineral smythite (ERD et al., 1957), which is not a thiospinel but a rhombohedral form related to the pyrrhotite structure.

CRYSTAL STRUCTURE

Thiospinels are modelled on the cubic oxide spinel structure in which sulphur atoms replace oxygen in approximately cubic close-packed arrangement (DE JONG and

HOOG, 1928; LUNDQVIST, 1943, 1947; SKINNER et al., 1964). The cubic unit cell contains eight AB_2S_4 formula units, and divalent and trivalent cations occupy tetrahedral A and octahedral B sites. When the divalent ions fill the A sites, the spinel-type is *normal*, whereas *inverse* spinels contain divalent cations in B sites and trivalent cations in both octahedral B and tetrahedral A sites. It has been established by X-ray and neutron diffraction studies that $CuCo_2S_4$ and all thiochromites are *normal* spinels (DE JONG and HOOG, 1928; LUNDQVIST, 1943; BOUCHARD et al., 1965), whereas indite is inverse (HAHN and KLINGER, 1950). Sometimes, the spinel structure is described in terms of a rhombohedral unit cell containing two AB_2S_4 units. In this setting, a parameter u defines the position of the sulphur atoms along the triad axis. In most structures, $u > 3/8$, the condition for ideal cubic close-packing of sulphur. As a result, the tetrahedral A sites are regular but the octahedral B sites show trigonal distortion along different [111] directions of the cubic unit cell. Each sulphur atom is four-coordinated to three cations in octahedral B sites located, for example, along [$\bar{1}00$], [$0\bar{1}0$] and [$00\bar{1}$] directions and one cation in a tetrahedral A site along [111]. To a first approximation sulphur ions form four sp^3 hybrid orbitals.

Various types of metal–metal interactions are possible and take place through sulphur intermediaries, provided there are unpaired electrons on the cations (DWIGHT and MEYNUK, 1968). Thus, B–B interactions involve 90° cation–anion–cation coupling, and A–B interactions involve 130° cation–anion–cation coupling. The strengths of these interactions, which affect the magnetic properties, are directly related to the degree of covalent mixing between cationic d orbitals and anionic s, p and d orbitals (GOODENOUGH, 1969).

ELECTRONIC CONFIGURATIONS, MOLECULAR ORBITALS AND BAND STRUCTURES OF THIOSPINELS

In ionic structures such as oxides and silicates, the electronic configurations of transition metal ions can be described by crystal field theory (BURNS, 1970). Table 2 summarizes the various electronic configurations acquired by ions of the transition elements in octahedral and tetrahedral coordinations. Ni^{2+}, Cr^{3+} and low-spin Co^{3+} and Fe^{2+} with half-filled and completely filled t_{2g} orbitals are particularly stable in octahedral coordination and acquire large octahedral site preference energies (DUNITZ and ORGEL, 1957; McCLURE, 1957). A similar situation applies to Co^{2+} and Ni^{3+} in tetrahedral coordination. High-spin Mn^{2+} and Fe^{3+} ions with completely

Table 2. Electronic configurations of transition metal ions

Number of 3d electrons	Cation	Octahedral coordination		Tetrahedral coordination	
		high-spin	low-spin	high-spin	low-spin
1	Ti^{3+}	$(t_{2g})^1$	$(t_{2g})^1$	$(e)^1$	$(e)^1$
2	V^{3+}	$(t_{2g})^2$	$(t_{2g})^2$	$(e)^2$	$(e)^2$
3	Cr^{3+}	$(t_{2g})^3$	$(t_{2g})^3$	$(e)^2(t_2)^1$	$(e)^3$
4	Mn^{3+}, Cr^{2+}	$(t_{2g})^3(e_g)^1$	$(t_{2g})^4$	$(e)^2(t_2)^2$	$(e)^4$
5	Fe^{3+}, Mn^{2+}	$(t_{2g})^3(e_g)^2$	$(t_{2g})^5$	$(e)^2(t_2)^3$	$(e^4)(t_2)^1$
6	Co^{3+}, Fe^{2+}	$(t_{2g})^4(e_g)^2$	$(t_{2g})^6$	$(e)^3(t_2)^3$	$(e^4)(t_2)^2$
7	Ni^{3+}, Co^{2+}	$(t_{2g})^5(e_g)^2$	$(t_{2g})^6(e_g)^1$	$(e)^4(t_2)^3$	$(e)^4(t_2)^3$
8	Ni^{2+}	$(t_{2g})^6(e_g)^2$	$(t_{2g})^6(e_g)^2$	$(e)^4(t_2)^4$	$(e)^4(t_2)^4$
9	Cu^{2+}	$(t_{2g})^6(e_g)^3$	$(t_{2g})^6(e_g)^3$	$(e)^4(t_2)^5$	$(e)^4(t_2)^5$
10	Zn^{2+}	$(t_{2g})^6(e_g)^4$	$(t_{2g})^6(e_g)^4$	$(e)^4(t_2)^6$	$(e)^4(t_2)^6$

half-filled 3d orbitals are stabilized relative to low-spin configurations by Hund's intraatomic exchange energies. In oxide spinels the 3d electrons tend to be localized on the cation. Magnetic interactions between localized electrons on neighboring cations lead to ferro- and antiferromagnetic coupling, which disappears at the Curie or Néel temperature. Such cationic A–B and B–B interactions account for the magnetic properties of oxide spinels.

In thiospinels, descriptions of the electronic configurations of transition metal ions are complicated by the possibilities that the 3d electrons may be either localized on the cation leading to spontaneous magnetism, collective without spontaneous magnetism, or transitional between these two extremes (GOODENOUGH, 1969). Molecular orbital and band theories of solids may be used to explain covalent bond formation with sulphur. In transition metal ions in the octahedral B sites, e_g group orbitals are vacated and, together with the 4s and 4p orbitals, overlap with filled 3s and 3p orbitals of the sulphur ions to form stable bonding σ_B molecular orbitals and unstable anti-bonding $\sigma_B{}^*$ orbitals (BURNS and VAUGHAN, 1970). Filled t_{2g} orbitals of the transition metal may remain non-bonding or form less stable π_B molecular orbitals by overlapping unoccupied π-bond forming orbitals of sulphur. In cations in the tetrahedral A sites, vacated (non-centro-symmetric) t_2 group orbitals form bonding σ_A and antibonding $\sigma_A{}^*$ molecular orbitals with sulphur, while the e group orbitals remain nonbonding. The σ_B and σ_A molecular orbitals constitute part of the valence band, while the $\sigma_B{}^*$ and $\sigma_A{}^*$ orbitals containing the antibonding $e_g{}^*$ and $t_2{}^*$ orbitals, belong to the conduction band. The transition metal 3d electrons are distributed over orbitals of the octahedral t_{2g}, tetrahedral e, and $\sigma_A{}^*$ and $\sigma_B{}^*$ groups to give electronic configurations analogous to those in Table 2.

Other effects complicate the picture. Because electrons are inefficient at screening the nuclear charge, 3d electrons become more stable and the cations less ionic through the transition elements to Zn. This leads to increased covalent mixing of metal and sulphur orbitals with rising atomic number, and lowering of the filled t_{2g} and e orbital levels into the valence band. Also the energy levels of the $\sigma_A{}^*$ and $\sigma_B{}^*$ molecular orbitals may coalesce or separate depending on the types of cation in the A and B sites and the extent of metal–sulphur bonding in each site. If there is an energy gap between the $\sigma_A{}^*$ and $\sigma_B{}^*$ bands, the thiospinel has semiconducting properties. The electrons tend to be localized and magnetic interactions through cation–sulphur–cation coupling lead to ferro-, antiferro- and ferrimagnetism. Alternatively, if the $\sigma_A{}^*$ and $\sigma_B{}^*$ bands coalesce they become collective electron states and the thiospinel has metallic properties including high electrical conductivity and temperature independent Pauli paramagnetism. Such behaviour occurs only when the antibonding orbitals are partially filled with 3d electrons (that is, the Fermi level lies in the conduction band). These two extremes of bonding may be illustrated by considering specific types of thiospinel.

1. Bonding in chromium spinels

Since Cr^{3+} has a high octahedral site preference energy all chromium spinels are normal with Cr^{3+} ions filling the B sites. Ferrimagnetism is observed in the thiochromites ACr_2S_4 in which A = Mn, Fe, Co and Zn (Table 4), and originates from antiferromagnetic coupling through 130° A–S–Cr interactions and 90° Cr–S–Cr

interactions. $CuCr_2S_4$ is ferromagnetic, and $NiCr_2S_4$ does not form a spinel phase but crystallizes with the cation–deficient, ordered nickel arsenide structure, which permits Ni^{2+} and Cr^{3+} each with high octahedral site preference energies to both occur in octahedral coordination. Thiochromites are semiconductors, except for $CuCr_2S_4$ which has metallic properties.

A schematic energy level diagram for the 3d orbitals in daubréelite is shown in Fig. 2. Since the relative stability of the 3d orbitals increases with rising atomic number, they are slightly more low-lying in iron than in chromium. However, the $t_{2g}-\sigma_B{}^*$ separation in Cr^{3+} is greater than the $e-\sigma_A{}^*$ separation in Fe^{2+} due to the increased metal-sulphur interaction in octahedral coordination. The α and β states refer to the spin directions of electrons in the orbitals. In high-spin Fe^{2+}, $3d^6$, the spin of the sixth electron is antiparallel (β) to the other five (α) occupying singly each of the 3d orbitals. The electrons in Cr^{3+}, $3d^3$, occupy each of the t_{2g} orbitals singly, and have parallel spins. The spins on adjacent Cr^{3+} ions, however, are antiparallel below the Curie temperature, $T_c = 192°K$. The energy gap between the $\sigma_A{}^*$ and $\sigma_B{}^*$ levels, although small in $FeCr_2S_4$ (GOODENOUGH, 1969) is sufficient to make daubréelite a semiconductor. However, the β-spin electron in tetrahedral Fe^{2+} is sufficiently delocalized to prevent Jahn-Teller distortion in $FeCr_2S_4$ (BURNS, 1970). These results conform with the Mössbauer spectra of daubréelite (Table 3). At 295°K no magnetic hyperfine splitting is observed but the isomer shift and quadrupole splitting are consistent with high-spin Fe^{2+} ions in a regular tetrahedral site. At 77°K, well below the Curie temperature, the spectrum shows magnetic hyperfine splitting and a magnetically induced quadrupole splitting. These parameters are contrasted with those of octahedral Fe^{2+} in indite in Table 3.

The energy gap between $\sigma_A{}^*$ and $\sigma_B{}^*$ levels increases in $CoCr_2S_4$ and $ZnCr_2S_4$ as a result of rising atomic number of the A site cation, so that these phases also have semiconducting and ferrimagnetic or antiferromagnetic properties. The energy gap

Table 3. Mössbauer parameters for iron in selected sulphide phases

Mineral	Types of iron	Temperature of spectrum (°K)	Isomer shift (mm/sec)	Quadrupole splitting (mm/sec)	Hyperfine magnetic field (k.gauss)	Reference
pyrite	low-spin octahedral Fe(II)	300	0·310	0·614	—	(a)
		81	0·403	0·620	—	(a)
violarite	low-spin octahedral Fe(II)	300	0·30	0·60	—	(b)
		77	0·31	0·64	—	(b)
daubréelite	high-spin tetrahedral Fe(II)	295	0·60	0	—	(c)
		77	0·72	0·17	206	(c)
indite	high-spin octahedral Fe(II)	295	0·88	3·27	—	(c)
		295	0·805	3·23	—	(d)
greigite	high-spin octahedral Fe(II)	4·2	0·70	0·30	322	(e)
	high-spin octahedral Fe(III)	4·2	0·45	0·40	465	(e)
	high-spin tetrahedral Fe(III)	4·2	0·40	0	486	(e)

(a) TEMPERLEY and LEFEVRE, J. Phys. Chem. Solids 27, 85 (1966).
(b) This work.
(c) GREENWOOD and WHITFIELD, J. Chem. Soc. A, 1697 (1968).
(d) EIBSCHUTZ et al., Phys. Lett. 24A, 563 (1967).
(e) VAUGHAN and RIDOUT (1970).

Table 4. Physical properties of thiospinels

Composition (mineral)	Number of antibonding electrons	Cell edge a(Å)	Electrical behaviour	Magnetic properties	Percent reflectivity ($\lambda = 589$ nm)	VHN (kg/mm²)	Thermal stability (°C)
$CuCo_2S_4$ (carrollite)	5	9·461[a]	M.[a]	P.p.[h]	44·5[j]	525-542[n]	---
Co_3S_4 (linnaeite)	3	9·399[a]	M.[a]	P.p.[t]	46·5-50·5[k]	450-613[j]	664[q] (D)
$(Co, Ni)_3S_4$ (siegenite)	4-5	9·418[a]	M.[a]	P.p.[h]	46·3-46·9[j]	471-579[n]	---
Ni_3S_4 (polydymite)	6	9·480[b]	---	---	42·8	330-384[k]	353[q] (D) ±3
$FeNi_2S_4$ (violarite)	4	9·463[b]	---	---	44·3-45·3[k]	241-373[l]	461[b] (D) ±3
$FeCr_2S_4$ (daubréelite)	3	9·989[c]	S.c.[a]	Fi.[c] ($T_c = 192°K$)	37-40[m]	---	1060[r] (T)
$MnCr_2S_4$	3	10·11[a]	S.c.[a]	Fi[h] ($T_c = 95°K$)	---	---	---
$ZnCr_2S_4$	6	9·986[a]	S.c.[a]	A-Fo[i]	---	---	---
$CoCr_2S_4$	3	9·916[c]	S.c.[a]	Fi[c] ($T_c = 220°K$)	---	---	---
$CuCr_2S_4$	5	9·629[d] 9·814[a]	M.[a]	Fo.[h]	---	---	---
Fe_3S_4 (greigite)	7	9·876[e]	S.c.[g]	Fi.[g]	38-43[o]	389-441[o] 312[p]	180-200[s] (D)
$NiFe_2S_4$	7	---	S.c.[g]	Fi.[g]	---	---	---
$FeIn_2S_4$	2	10·62[f]	---	---	27-28[f]	309[f]	---

M. metallic; S.c. semi-conductor; P.p. Pauli paramagnetic; Fo. ferrimagnetic; A-Fi. antiferromagnetic; Fo. ferromagnetic; T_c Curie Temperature   D decomposition temperature   T transition temperature

a BOUCHARD et al. (1965)
b CRAIG (1967)
c SHICK and VON NEIDA (1969)
d MAHN et al. (1956)
e SKINNER et al. (1964)
f GENKIN and MURAVIEVA (1963)
g HULLIGER (1968)
h GOODENOUGH (1969)
i LOTGERING (1968)
j McLEOD and CHAMBERLAIN (1968)
k This work
l PETRUK et al. (1969)
m CAVE et al. (1969)
n YOUNG and MILLMAN (1964)
o KRAMM and SUKHITSKAYA (1965)
p RADUSONOVIĆ (1966)
q KULLERUD (1968)
r ALBERS and ROOYMANS (1965)
s UDA (1967)
t HEIDELBERG et al. (1966)

is also higher in $MnCr_2S_4$ than in $FeCr_2S_4$ because of the high intra-atomic exchange energy of Mn^{2+}.

Thus, the substitution of Mn and Zn for Fe in meteoritic daubréelites is readily explained: they all occur in the A-site and have similar band structures and hence physical properties. One would predict small amounts of Co and Cu, but negligible Ni, to occur in natural daubréelites.

2. Bonding in Co–Ni–Cu thiospinels

Figure 1 shows that extensive solid-solution appears to exist in the linnaeite–siegenite–polydymite series. The complete miscibility of Co_3S_4 and Ni_3S_4 is predicted by band theory. The synthetic phases Co_3S_4, $NiCo_2S_4$ and $CoNi_2S_4$ have been shown
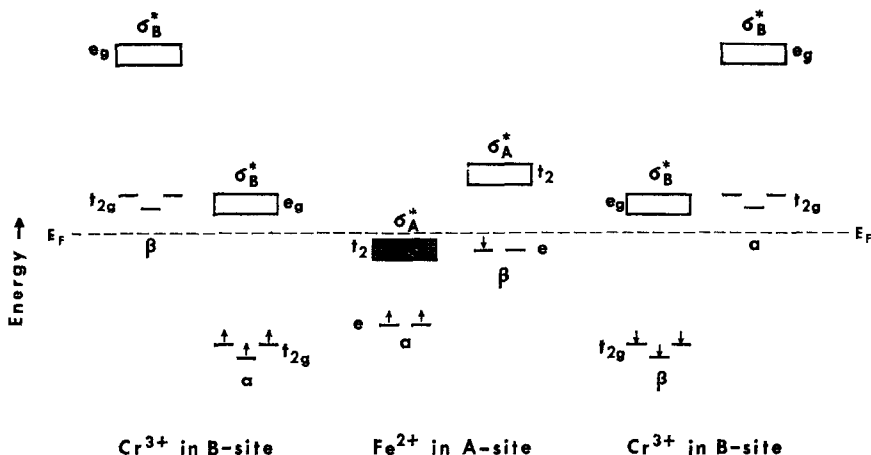
Fig. 2. Schematic energy level diagram for the 3d orbitals in $FeCr_2S_4$ (after GOODENOUGH, 1967). α and β refer to spin directions of electrons; E_F is the Fermi level. The diagram applies below the Curie temperature, $T_c = 192°K$.

to possess metallic properties (BOUCHARD *et al.*, 1965), and the schematic energy level diagram shown in Fig. 3 has been suggested for Co_3S_4 (GOODENOUGH, 1967, 1969). The high octahedral site preference energy of low-spin Co^{3+} and the stability of Co^{2+} in tetrahedral coordination leads to the prediction that Co_3S_4 is a normal spinel with the formal cation distribution $Co^{2+}[Co^{3+}]_2S_4$. Note, however, that in compounds posessing metallic properties, it is meaningless to assign formal valencies to the cations (GOODENOUGH, 1969). The valence band t_{2g} and e levels are completely filled and the antibonding levels, capable of accommodating 14 electrons per Co_3S_4 formula unit, contain only three 3d electrons. The metallic properties indicate that the $\sigma_B{}^*$ and $\sigma_A{}^*$ bands overlap, but the weak temperature dependent paramagnetism suggests that the σ^* band is narrow (GOODENOUGH, 1969).

Substitution of nickel for cobalt leads to the compositions $Co_{3-x}Ni_xS_4$ and an increase from 3 to $(3 + x)$ electrons per molecule in the σ^* band. Neutron diffraction
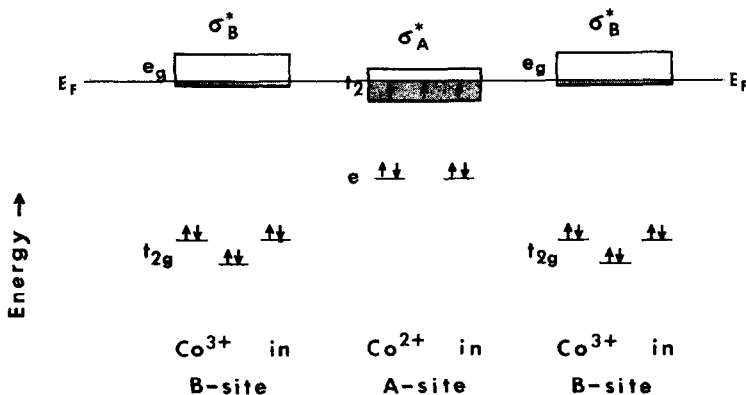

Fig. 3. Schematic energy level diagram for the 3d orbitals in Co_3S_4 (after GOODENOUGH, 1967, 1969). E_F is the Fermi level.

4

data indicate that $NiCo_2S_4$ is a normal spinel (GOODENOUGH, 1967) and that each A-site Ni^{2+} ion therefore contributes 4 electrons to the σ^* band. The Jahn–Teller distortion predicted for tetrahedral Ni^{2+} (BURNS, 1970) is offset by electron delocalization in the σ^* band. In Ni_3S_4, there are 6 electrons in the σ^* band and, since Ni^{2+} has a high octahedral site preference energy, this thiospinel is predicted to be inverse with a formal cation distribution $Ni^{3+}[Ni^{2+}Ni^{3+}]S_4$. Again, the Jahn–Teller distortion expected for octahedrally coordinated low-spin Ni^{3+} ions (BURNS, 1970) is offset by electron delocalization in the σ^* band, although in such a metallic compound assignment of formal valencies to the cations is arbitrary. Thus, the existence of the linnaeite–siegenite–polydymite solid-solution series is readily explained by this band model: nickel substituting for cobalt in Co_3S_4 does not fundamentally alter the band structure but merely leads to a raised Fermi level as a result of introducing more electrons into the antibonding levels.

The carrollite–linnaeite solid-solution series may be similarly explained. In $CuCo_2S_4$, which is a normal spinel (DE JONG and HOOG, 1928), low-spin Co^{3+} occupies octahedral B sites and Cu^{2+} ions occupy tetrahedral A sites. Jahn–Teller distortion of the thiospinel structure would occur if the 3d electrons were localized on Cu^{2+} (BURNS, 1970). The absence of such distortion and the metallic properties of $CuCo_2S_4$ (Table 4) may again be attributed to delocalization of these electrons in the σ^* band. Therefore, mixed crystal compositions $Cu_xCo_{3-x}S_4$ contain $(3 + 2x)$ electrons in the σ^* band, which is thus 5/14 filled in $CuCo_2S_4$. No compositions richer in copper than $CuCo_2S_4$ are possible, as this would imply the existence of the Cu(III) oxidation state, which is very unstable.

It is also possible by the band model to account for possible metallic properties of $FeNi_2S_4$ and the existence of the polydymite–violarite solid–solution series. The Mössbauer spectrum of violarite at 77°K (Table 3) consists of a doublet with a small isomer shift and quadrupole splitting. The slight asymmetry sometimes observed in the low velocity region may be attributed to small amounts of Fe^{3+} ions in A sites. The similarity of the Mössbauer parameters of violarite to those of iron in pyrite suggests that octahedrally coordinated, low-spin Fe^{2+} occurs in violarite, which is, therefore, an inverse spinel $Ni^{3+}(Fe^{2+}Ni^{3+})S_4$. Such distribution conforms with the large octahedral site preference energy of low-spin Fe^{2+} and the stability of Ni^{3+} in tetrahedral sites. Substitution of Ni^{2+} by Fe^{2+} in the polydymite–violarite series $Fe_xNi_{1-x}^{2+}Ni_2^{3+}S_4$ thus leads to a reduced number of 3d electrons in the σ^* band from six in Ni_3S_4 to four in $FeNi_2S_4$.

3. *Bonding in iron thiospinels*

Greigite, Fe_3S_4, has ferrimagnetic and semiconducting properties (HULLIGER, 1968). In this respect, it resembles daubréelite rather than violarite, suggesting that the nature of the iron cations in greigite and violarite differ. The Mössbauer spectrum of greigite is complex, but at 4·2°K it has been resolved into three sets of six-line magnetic hyperfine spectra (VAUGHAN and RIDOUT, 1970). These are attributed to high-spin Fe^{3+} ions in tetrahedral A sites and octahedral B sites and high-spin Fe^{2+} ions in octahedral B sites. The isomer shift and quadrupole splitting (Table 3) are consistent with high-spin Fe^{2+} ions in the trigonally distorted B sites of the spinel structure. Thus, greigite is an inverse spinel $Fe^{3+}[Fe^{2+}Fe^{3+}]S_4$ and is therefore the

sulphur analogue of magnetite Fe_3O_4. The lack of solid-solution between $FeNi_2S_4$ and Fe_3S_4 (Fig. 1) is readily explained by the different spin states of octahedrally co-ordinated Fe^{2+}: low-spin Fe^{2+} ions occur in violarite which is metallic, whereas high-spin Fe^{2+} ions occur in greigite which is semiconducting.

The nickel analogue of greigite, $NiFe_2S_4$, is documented as having semiconducting and ferrimagnetic properties (HULLIGER, 1968). It is also predicted to be an inverse spinel $Fe^{3+}[Ni^{2+}Fe^{3+}]S_4$ since Ni^{2+} has a high octahedral site preference. Solid-solution is predicted, therefore, along the Fe_3S_4–$NiFe_2S_4$ series. However, although $NiFe_2S_4$ and $CuFe_2S_4$ are catalogued as thiospinels, $CoFe_2S_4$ and $MnFe_2S_4$ have been documented as doubtful synthetic thiospinel phases (HULLIGER, 1968). Thus, naturally occurring greigites might be expected to contain small amounts of nickel (RADUSINOVIĆ, 1966) and copper, but negligible cobalt and manganese.

PHYSICAL PROPERTIES OF THIOSPINELS

1. *Cell parameters*

Although crystal structure determinations have been made on comparatively few compositions, unit cell data are available for most natural and synthetic thiospinel and analogous compounds. Those pertaining to minerals discussed in this paper are summarized in Table 4. The cell sizes group into two categories: those greater than 9·85 Å and those smaller than 9·50 Å.

LOTGERING (1956) has pointed out that if the spinel structure contained ionic sulphurs in cubic close packing, the cell edge should be $> 9·85$ Å, resulting from S^{2-} ions in contact. Smaller distances are indicative of appreciable covalency.

The cell edges shown in Table 4 are consistent with the descriptions of chemical bonding and electronic configurations discussed earlier. The comparatively large values for thiochromites are consistent with the belief that 3d electrons are localized on Cr^{3+} and the A site cations. Only in $CuCr_2S_4$ is the cell edge significantly smaller which may be correlated with this composition having different electrical and magnetic properties than the other thiochromites (Table 4).

The small cell edges in thiocobaltites and thionickelites may be correlated with the high degree of covalency in these phases, resulting from low-spin configurations of octahedrally coordinated cations. Thus, the cell edge is smallest in Co_3S_4, which also has the smallest number of electrons in antibonding σ^* orbitals. With increasing electron occupancy of the antibonding orbitals in the Co_3S_4–Ni_3S_4 and Co_3S_4–$CuCo_2S_4$ series, the cell size increases significantly. Even the small contraction in the Ni_3S_4–$FeNi_2S_4$ series is consistent with a decreased occupancy of the σ^* band. A similar expansion of cell edge is observed in pyrite-type compounds, in which progressive expansion of the cell from FeS_2 through CoS_2 to NiS_2 is the result of increased electron occupancy of σ^* orbitals. It may be noted that the large cell size of greigite compared to violarite is a further indication of the different character of Fe^{2+} ions in these two minerals.

2. *Microhardness*

In pyrite-type compounds decreasing values of the microhardness along the series FeS_2–CoS_2–NiS_2 may be correlated with increasing cell size (NICKEL et al., 1970; DEMIRSOY, 1969; VAUGHAN, 1969). A similar trend is also shown in thiospinels

(Table 4), although the literature data on these minerals are sparce and confused. Frequently, thiospinels occur as supergene phases in complex intergrowths with shrinkage cracks, which render polished section mounts difficult to prepare for microhardness (and reflectivity) measurements. Nevertheless, there is a consistent trend towards decreasing microhardness values with increasing cell size resulting from increased occupancy of the antibonding levels in the linnaeite–polydymite and linnaeite–carrollite series.

There is no good correlation between microhardness and cell size when the correlation is extended to greigite and daubréelite, possibly because the 3d electrons are more localized in these "ionic" phases. However, it is significant that the high pressure polymorph of $FeCr_2S_4$ with a defect nickel arsenide structure is harder to abrade and more strongly reflecting than the thiospinel phase (EL GORESY et al., 1968). Both properties correlate with the increased density and hence decreased cell parameters of the high pressure polymorph.

3. *Reflectivity*

The available reflectivity values for the thiospinel minerals are summarized in Table 4. There is a noteworthy trend of decreasing reflectivity along the linnaeite–polydymite series (PONOMAREVA, 1965) and the linnaeite–carrollite series, which may be correlated with increased occupancy of the antibonding σ^* orbitals. BURNS and VAUGHAN (1970) have shown that there is a direct correlation between per cent reflectivity and effective number of free electrons in pyrite-type compounds. The values of the effective number of free electrons are roughly proportional to the number of energy levels available to t_{2g} electrons excited into antibonding e_g^* orbitals, and decrease along the series FeS_2–CoS_2–NiS_2–CuS_2. The effective numbers of free electrons have not been calculated for thiospinels. However, by analogy with the pyrite group, reflectivities of thiospinels are predicted to decrease along the series Co_3S_4–Ni_3S_4, Co_3S_4–$CuCo_2S_4$, and $FeNi_2S_4$–Ni_3S_4 in which the number of available levels in antibonding orbitals for electron excitation also decrease. The reflectivity data in Table 4 are in excellent agreement with these predictions.

Substitution of sulphur by selenium in thiospinels is predicted to cause higher reflectivity, by analogy with the pyrite-type compounds (BURNS and VAUGHAN, 1970). This prediction is substantiated by the data for trüstedtite, which show it to have a higher reflectivity than $Ni_3(Se, S)_4$ solid-solutions (VUORELAINEN et al., 1964).

THERMAL STABILITIES AND GEOLOGICAL OCCURRENCES OF THE THIOSPINELS

The previous section has demonstrated some of the correlations that exist between certain physical properties and the electronic structures of thiospinels. Phase equilibria studies of several sulpho-spinels have been made and the relative stabilities, and hence geological occurrences of thiospinels may also be explained by band and molecular orbital theories. High pressure transformations are discussed in the following section. Here, the thermal stabilities of thiospinels at low pressures will be considered.

KULLERUD (1968) showed that at elevated temperatures M_3S_4-type compounds decompose to a mixture of monosulphides and di-sulphides. Linnaeite breaks down

at 664°C to hexagonal $Co_{1-x}S$ plus cubic CoS_2, whereas the corresponding nickel compounds are formed from polydymite at 356°C. CRAIG (1967), who demonstrated the existence of solid-solution between Ni_3S_4 and $FeNi_2S_4$ above 300°C, showed that violarite is stable up to 461°C. Studies of synthetic Fe_3S_4 by UDA (1967) indicate that greigite breaks down to pyrrhotite at temperatures between 180°C and 200°C. Thermal studies of $FeCr_2S_4$ suggest that it melts congruently (KULLERUD, 1968) and that the spinel form of daubréelite transforms to a high pressure polymorph at 1060°C (ALBERS and ROOYMANS, 1967; BELL et al., 1969).

The thermal stability data are summarized in Table 4. The results show that in Co–Ni–Fe thiospinels, the relative stabilities decrease in the order Co_3S_4–$FeNi_2S_4$–Ni_3S_4–Fe_3S_4. This order is also that of increasing number of electrons in antibonding molecular orbitals. Thus, the relative stability of a thiospinel mineral is related to transition metal cations in low-spin states possessing small numbers of antibonding electrons. The high stability of daubréelite is attributed to the large octahedral site preference energy of Cr^{3+} ions in the B-sites of the spinel structure. One would predict from these correlations that siegenites and carrollite with four or five electrons in antibonding orbitals would have thermal stabilities intermediate between linnaeite and polydymite.

These stability relations are reflected in the geological occurrences of thiospinels (Table 1). Thus, daubréelite occurs in high temperature assemblages in meteorites. The relatively high stability of linnaeite accounts for its widespread distribution in both stratiform copper deposits and hydrothermal vein assemblages. Carrollite and siegenites apparently tend to appear in the low-temperature stratiform copper deposits (carrollite) or low-temperature complex sulphide deposits such as the zinc–lead–copper deposits at Fredrickstown (siegenite). The literature is not entirely unambiguous or unanimous with respect to the origin of many of the deposits in which these minerals occur, but there does appear to be a tendency for linnaeite to occur in higher temperature assemblages and for carrollite and siegenites to be restricted to lower temperature environments.

The relatively lower stabilities of violarite and polydymite correlate with their most commonly reported occurrences as supergene secondary minerals. Polydymite, however, has also been reported as a primary mineral. The low stability of greigite accounts for its occurrence in recent low temperature sedimentary environments. The transient formation of greigite in muds and vegetable debris suggests that it may have been an important intermediary in the formation of sedimentary iron sulphide ore deposits.

In summary, the stabilities acquired by individual transition metal ions in octahedral coordination and low-spin states in the thiospinel structure explains the relative stabilities and hence geological occurrences of the thiospinel minerals.

HIGH PRESSURE TRANSFORMATIONS OF THIOSPINELS

Synthetic ternary sulphides AB_2S_4 of the transition elements adopt either the spinel or a cation deficient nickel arsenide structure (TRESSLER et al., 1968). The relationship between these two structures is important in connection with possible phase transitions in shocked meteorites and within the earth's interior.

The defect nickel arsenide structure is of two types: a hexagonal structure in

which the cations and vacancies are disordered; and a monoclinic Cr_3S_4 structure in which the A^{2+} cations and vacancies occupy the same plane and the B^{3+} ions occupy filled alternate planes perpendicular to the c axis (for example, $NiCr_2S_4$, ANDRON and BERTAUT, 1966). The differences between the spinel structure and the cation defective NiAs structure are major (TRESSLER *et al.*, 1968); spinels have approximately cubic close-packing of sulphurs, whereas the sulphurs are approximately hexagonally close-packed in the NiAs structure; cations are both four- and six-coordinated in spinel, but only six-coordinated by sulphur in the NiAs structure; and octahedra are edge-shared in the spinel structure but face-shared in the NiAs structure. These factors indicate that the defect NiAs structure will be the more dense, and that spinel → defect NiAs transformations may take place at elevated pressures.

ALBERS and ROOYMANS (1965) and ROOYMANS and ALBERS (1965) studied the transition of $FeCr_2S_4$ to a polymorph with the hexagonal defect NiAs structure. Their equilibrium diagram has a negative slope of about 38·5 atm per degree and shows that the transition takes place in $FeCr_2S_4$ at 20 kbar, 525°C and 1 bar, 1060°C. BOUCHARD (1967) confirmed that high pressure polymorphism occurs in $FeCr_2S_4$, but succeeded in synthesising the monoclinic, ordered defect NiAs polymorph. The density of both high pressure polymorphs is about 8% higher than that of daubréelite. The DTA measurements of BELL *et al.* (1969) on a natural daubréelite may indicate the stability fields of the two high pressure polymorphs. BOUCHARD (1967) also demonstrated that the transition pressures at 600°C decrease in the order $MnCr_2S_4$ > $FeCr_2S_4$ = $CoCr_2S_4$ > $NiCr_2S_4$ (which has the defect NiAs structure at P = 1 atm). No transformation could be induced in $CuCr_2S_4$ and $ZnCr_2S_4$ within the limits (80 kbar) of the apparatus.

Subsequently, several chalcogenide phases have been shown to undergo spinel → defect NiAs structure transitions at elevated pressures (EL GORESY *et al.*, 1968; TRESSLER *et al.*, 1968). KULLERUD (1968) has demonstrated that polydymite, linnaeite, violarite, carrollite, siegenite, bornhardtite and trüstedtite also transform to defect NiAs structures at elevated pressures and temperatures. In fact cubic and monoclinic Ni_3Se_4 phases coexist as the minerals trüstedtite and wilkmanite in uranium-bearing albitite dykes (VUORELAINEN *et al.*, 1964). In polydymite the transition occurs at pressures between 450 and 400 bars and temperatures between 250 and 356°C, whereas in linnaeite an inversion point is observed at 2·5 kbar and 640°C. It is significant that such transitions occur only in thiospinels in which A site and B site cations have unfilled 3d orbitals (TRESSLER *et al.*, 1968), and are extremely difficult in compounds such as $ZnCr_2S_4$ in which cations are stabilized in tetrahedral A sites relative to octahedral coordination.

The geophysical significance of the thiospinel to defect NiAs structure transitions is obvious (ALBERS and ROOYMANS, 1965). First, daubréelite and other thiospinels are predicted to undergo polymorphic transitions in the Crust or Upper Mantle at depths proportional to the zinc content, and to exist as the denser defect NiAs structure polymorph in the Mantle. Second, shock metamorphism of meteorites should include spinel → defect NiAs structure transitions in daubréelite. Such transitions may account for the observation that certain daubréelite phases in stony meteorites show textural evidence to suggest that they once had a hexagonal structure (RAMDOHR, 1963; EL GORESY *et al.*, 1968).

REFERENCES

ALBERS W. and ROOYMANS C. J. M. (1965) High pressure polymorphism of spinel compounds. *Solid-St. Commun.* **3,** 417–419.

ANDREWS R. W. (1962) *Cobalt.* Minerals Resources Division, Overseas Geological Surveys Publ. 222 pp.

ANDRON N. and BERTAUT E. F. (1966) Étude par diffraction neutronique de Cr_2NiS_4. *J. Phys.* **27,** 619–626.

BELL P. M., EL GORESY A., ENGLAND J. L. and KULLERUD G. (1969) Pressure–temperature diagram for Cr_2FeS_4. *Carnegie Inst. Wash., Ann. Rept.,* **68,** 277–278.

BIRD W. H. (1969) A note on the occurrence of violarite, Copper King Mine, Boulder County, Colorado. *Econ. Geol.* **64,** 91–94.

BOUCHARD R. J. (1967) Spinel to defect NiAs structure transformation. *Mat. Res. Bull.* **2,** 459–464.

BOUCHARD R. J., RUSSO P. A. and WOLD A. (1965) Preparation and electrical properties of some thiospinels. *Inorg. Chem.* **4,** 685–688.

BURNS R. G. (1970) *Mineralogical Applications of Crystal Field Theory.* Cambridge Univ. Press.

BURNS R. G. and VAUGHAN D. J. (1970) Interpretation of the reflectivity behavior of ore minerals. *Amer. Mineral.* **55,** 1576–1586.

CAYÉ R., GIRAUD R. and SANDREA A. (1969) Phase métallique des météorites pierreuses. In *Meteorite Research* (editor P. M. Millman), pp. 657–668. D. Reidel.

CORNWALL H. R. (1966) Nickel deposits of North America. *U.S. Geol. Surv., Bull.* 1223, 62 pp.

CRAIG J. R. (1967) The Fe–Ni–S system: violarite stability relations. *Carnegie Inst. Wash., Ann. Rept.* **66,** 434–436.

DE JONG W. F. and HOOG A. (1928). Carrollite (sychnodymite). *Z. Krist. allogr.* **66,** 168–171.

DEMIRSOY S. (1969) Untersuchungen über den Einfluss der chemischen Zusammensetzung auf die Spektralen Reflexionsfunktionen und Mikroeindruckhärten im System FeS_2–NiS_2–CoS_2, an Zonen eines naturlichen Bravoit-Kristalls. *Neues Jahrb. Mineral., Monatsh.* **17,** 323–333.

DWIGHT K. and MENYUK N. (1968) Analysis of distant-neighbour interactions in cubic spinels. *J. Appl. Phys.* **39,** 660–661.

DUNITZ J. D. and ORGEL L. E. (1957) Electronic properties of transition element oxides. II. Cation distribution amongst octahedral and tetrahedral sites. *J. Phys. Chem. Solids* **3,** 318–333.

EIBSCHUTZ M., HERMAN E. and SHTRIKMAN S. (1967) Determination of cation valencies in $Cu_2{}^{57}Fe^{119}SnS_4$ by Mössbauer effect and magnetic susceptibility measurements. *J. Phys. Chem. Solids* **28,** 1633–1636.

EL GORESY A. (1967) Quantitative electron microprobe analysis of coexisting sphalerite, daubréelite and troilite in the Odessa iron meteorite and their genetic implications. *Geochim. Cosmochim. Acta* **31,** 1667–1676.

EL GORESY A., BELL P. M. and ENGLAND J. L. (1968) Synthesis of β-Cr_2FeS_4 at 35 kb. *Carnegie Inst. Wash., Ann. Rept.* **67,** 197–198.

EL GORESY A. and KULLERUD G. (1969) Phase relations in the system Cr–Fe–S. In *Meteorite Research* (editor P. M. Millman), pp. 638–656. D. Reidel.

ERD R. C., EVANS H. T. JR. and RICHTER D. H. (1957) Smythite, a new iron sulphide, and associated pyrrhotite from Indiana, *Amer. Mineral.* **42,** 309–333.

FLEISCHER M. (1966) Index of new mineral names, discredited minerals, and changes of mineralogical nomenclature of volumes 1–50 of *The American Mineralogist. Amer. Mineral* **51,** 1247–1357.

FRENZEL G. and OTTEMAN J. (1968) Über ein neues NiAs mineral und eine bemerkenswerte Uranmineralisation von der Anna–Procopi–Grube bei Pribaum. *Neues Jahrb. Mineral., Monatsh.* **11,** 420–429.

GENKIN A. D. and MURAV'EVA I. V. (1963) Indite and jalindite, new indium minerals. *Zap. Vses. Mineral., Obshchest.*, **92**, 445–457.

GODDARD E. N. and LOVERING T. S. (1942) Nickel deposit near Gold Hill, Boulder County, Colorado. *U.S. Geol. Surv., Bull.* 931–0, 15 pp.

GOODENOUGH J. B. (1967) Description of transition metal compounds: application to several sulphides. In *Propriétés thermodynamiques physiques et structurales des dérives semi-métalliques.* Ed. du Center National de la Recherche Scientifique, no. 157, p. 263–292.

GOODENOUGH J. B. (1969) Descriptions of outer d electrons in thiospinels. *J. Phys. Chem. Solids* **30**, 261–280.

GREENWOOD N. N. and WHITFIELD H. J. (1968) Mössbauer effect studies on cubanite ($CuFe_2S_3$) and related iron sulphides. *J. Chem. Soc.* A, 1697–1699.

HACH-ALI P. F. and OTTEMANN J. (1967) Linneit und Bravoit von Fredericktown, Missouri. *Der Aufschluss* **1**, 29–33.

HAHN H., DELORENT C. and HARDER B. (1956). Ternary chalcogenides. VIII. The structure of CuV_2S_4, $CuCr_2S_4$, $CuCr_2Se_4$ and $CuCr_2Te_4$. *Z. anorg. allgem. Chem.* **283**, 138–142.

HAHN H. and KLINGER W. (1950) Über die Kristallstruktur einiger ternärer Sulfide, die sich vom Indium (III)-sulfide albeiten. *Z. anorg. Chem.* **263**, 177–190.

HAWLEY J. E. (1962) The Sudbury ores: their mineralogy and origin. *Canad. Mineral.* **7**, 1–207.

HEIDELBERG R. F., LUXEM A. H., TALHOUK S. and BANEWICZ J. J. (1966) The magnetic susceptibilities of the cobalt–sulphur system. *Inorg. Chem.* **5**, 194–197.

HEY M. H. (1962) *An Index of Mineral Species and Variations.* British Museum Publ.

HOFFMAN V., KUPA K. and TRDLICKA Z. (1963) Polydymite, a new mineral for Czechoslovakia. *Sb. Narod. Musea Praze* **19B**, 103–115.

HULLIGER F. (1968) Crystal chemistry of the chalcogenides and pnictides of the transition elements. *Structure and Bonding* **4**, 83–299.

JEDWAB J. (1967) Mineralization of vegetable debris in a recent mud to greigite. *Bull. Soc. Belge. Geol.* **26**, 27–38.

KATITSYN Y. V. (1959) Copper linnaeite from Eastern Siberia. *Mat. Vses. Nauk.-Issled., Geol. Inst.* **26**, 66–71.

KEIL K. (1968) Zincian daubréelite from the Kota–Kota and St. Mark's enstatite chondrites. *Amer. Mineral.* **53**, 491–495.

KEIL K. and FREDRIKSSON F. (1963) Electron microprobe analysis of some rare minerals in the Norton County achondrite. *Geochim. Cosmochim. Acta* **27**, 939–947.

KRAMM T. P. and SUKHITSKAYA N. Yu. (1965) Melnikovite from the Kimmerian sediments of the Kerch peninsula. *Min. Sborn. L'vov Univ.* **19**, 520–523.

KULLERUD G. (1968) Cubic-hexagonal inversions in some M_3S_4-type sulphides. *Carnegie Inst. Wash., Ann. Rept.* **67**, 179–182.

LOTGERING F. K. (1956) On the ferrimagnetism of some sulphides and oxides. *Philips Res. Rept.* **11**, 218–249; 337–350.

LOTGERING F. K. (1968) Mixed crystals between binary sulphides and selenides with spinel structure. *J. Phys. Chem. Solids* **29**, 699–709.

LUNDQVIST D. (1943) Crystal structure of daubréelite. *Arkiv. Kemi, Mineral., Geol.* **17B**, No. 12. 4 pp.

LUNDQVIST D. (1947) X-ray studies on the ternary system Fe–Ni–S. *Arkiv Kemi, Mineral., Geol.*, **24A**, No. 22, 12 pp.

McCLURE D. S. (1957) The distribution of transition metal cations in spinels. *J. Phys. Chem. Solids* **3**, 311–317.

McLEOD C. R. and CHAMBERLAIN J. A. (1968) Reflectivity and Vickers microhardness of ore minerals. Chart and tables. *Geol. Surv. Canada,* paper 68–64.

NICKEL E. H., WEBSTER A. H. and RIPLEY L. (1970) Bond strengths in the disulphides of iron, cobalt and nickel. In preparation.

PERMINGEAT F. and WEINRUB E. (1960) Sur des inclusions cobaltiferèus dans la chalcopyrite d'Azegour (Maroc). *Bull. Soc. franc., Min. Cristallogr.*, **88**, 63–66.

PETRUK W., HARRIS D. C. and STEWART J. M. (1969) Langisite, a new mineral, and the rare minerals cobalt pentlandite, siegenite, parkerite and bravoite from the **Langis Mine**, Cobalt–Gowganda area, Ontario. *Can. Mineral.* **9**, 597–616.

POLUSHKINA A. P. and SIDORENKO G. A. (1963) Melnikovite as a mineral species. *Zap. Vses. Mineral., Obshch.* **92,** 547–554.

PONOMAREVA M. N. (1965) Reflectivity of some sulphides and similar compounds. *Min. Sborn. L'vov Univ.* **19,** 506–508.

POWELL H. E. (1967) Magnetic susceptibility of 19 nickel and cobalt-bearing minerals. *U.S. Bur. Mines, Info. Circ.* No. 8351. 12 pp.

RADUSINOVIĆ D. S. (1966) Greigite from the Lojane chromium deposit, Macedonia. *Amer. Mineral.* **51,** 209–215.

RAMDOHR P. (1963) The opaque minerals in stony meteorites. *J. Geophys. Res.* **68,** 2011–2036.

ROOYMANS C. J. M. and ALBERS W. (1963) High pressure polymorphism of $FeCr_2S_4$ and related compounds. In *Propriétés thermodynamiques physiques et structurales des dérives semi-métalliques.* Ed. du Centre National de la Recherche Scientifique, No. 157, p. 63–66.

SHICK L. K. and VON NEIDA A. R. (1969) Single crystal growth of $CoCr_2S_4$ and $FeCr_2S_4$. *J. Cryst. Growth* **5,** 313–314.

SKINNER B. J., ERD R. C. and GRIMALDI F. S. (1964) Greigite, the thiospinel of iron; a new mineral. *Amer. Mineral.* **49,** 543–555.

SNYDER F. G. and GERDEMANN P. E. (1969) Geology of S. E. Missouri lead district. In *Ore Deposits in the U.S., 1933–1967,* (editor J. D. Rodge), Part 3, Chap. 17.

TARR W. A. (1935) The linnaeite group of cobalt–nickel–iron–copper sulphides. *Amer. Mineral.* **20,** 69–80.

TEMPERLEY A. A. and LE FEVRE H. W. (1966) The Mössbauer effect in marcasite structure iron compounds. *J. Phys. Chem. Solids* **27,** 85–92.

TRESSLER R. E., HUMMEL F. A. and STUBICAN V. S. (1968) Pressure–temperature study of sulfospinels. *J. Amer. Ceram. Soc.* **51,** 648–651.

UDA M. (1967) The structure of synthetic Fe_3S_4 and the nature of the transition to FeS. *Z. anorg. allgem. Chem.* **350,** 105–109.

VAUGHAN D. J. (1969) Zonal variation in bravoite. *Amer. Mineral.* **54,** 1075–1083.

VAUGHAN D. J. and RIDOUT, M. S. (1970) Mössbauer study of some sulphide minerals. *J. Inorg. Nucl. Chem.* In press.

VOKES F. M. (1967) Linnaeite from the Precambrian Raipas Group of Finnmark, Norway. *Mineral. Deposita* **2,** 11–25.

VUORELAINEN Y., HUHMA A. and HÄKLI A. (1964) Sederholmite, wilkmanite, kullerudite, mäkinenite and trüstedtite, five new nickel selenide minerals. *Bull. Comm. Geol. Finlande* **36,** 113–126.

YOUNG B. B. and MILLMAN A. P. (1964) Microhardness and deformation characteristics of ore minerals. *Trans. Inst. Min. Metall.* **73,** 437–466.